Tuijin Jishu/Journal of Propulsion Technology
ISSN:1001-4055
Vol. 44 No.4 (2023)

Mathematical and Computational Fluid Dynamics Analysis of Low-Altitude Rocket Static Stabilityfor Various Fin Designs

[1,2] Alif Abni Bin Adnan, [1,2] Ahmad Hussein Bin Abdul Hamid, [1,2] Zuraidah Salleh, [1,2] Muhammad Zakwan Azizi, [2,3] Mohamad Amirul Muhammad

[1] School of Mechanical Engineering, College of Engineering, Universiti Teknologi MARA (UiTM),Shah Alam campus, Selangor, [2] High Energy Material Research Laboratory (HEMREL), College of Engineering, Universiti Teknologi MARA (UiTM), Shah Alam campus, Selangor, [3] MTC Defence, MTC Engineering Sdn Bhd. Jalan Teknokrat 2, Zon Teknologi MKN Embassy, Cyberjaya 63000 Sepang, Selangor

Abstract—Rocket fins play an important role in determining theirstability during flight. The key characteristics that determine the static stability of a rocket are the relative positions of its centre of gravity and centre of pressure.Determining the centre of gravity is rather simple. However, determining the centre of pressure is more challenging as it depends on the pressure distribution over the surface of the entire rocket body. The present study analyses the static stability of a low-altitude rocket with various fin designs.The parameter used to measure the aerodynamic stability of the rocket is the static margin, Me.Mathematical predictionsusing Barrowman equations and computational fluid dynamics(CFD) were employed to obtain data for the centre of pressure and centre of gravity. The data from both approaches was then compared and analysed. The Barrowman equations were shown to provide support for the computational fluid dynamicsdata, indicating that the static margin is determined by the centre of pressure. However, there are differences in terms of the observed trend.

Index Terms—*centre of gravity, centre of pressure, CFD analysis, rocket fin, stability, static stability, static margin.*

Introduction

A low-altitude rocket has received considerable attention due to its various applications. The applications of low-altitude rockets are like those of sounding rockets[1][2][3][4][5]: experimental study, weather study, and modification (cloud seeding)[6]. The rocket may be subject to instability, which depends on the location of the centre of pressure and centre of gravity of the rocket. Stability is the tendency of a system to return to or recover from its original condition after facing perturbation, as well as the ability of the rocket to keep flying in the right direction without wobbling or tumbling. The parameter used to measure the aerodynamic stability of the rocket is the static margin, Me, defined in equation(1).Fig. 1 shows an illustration of the aerodynamic stability of rocket flight.

$$\mathrm{Me} = \frac{C_P - C_G}{d}, \qquad (1)$$

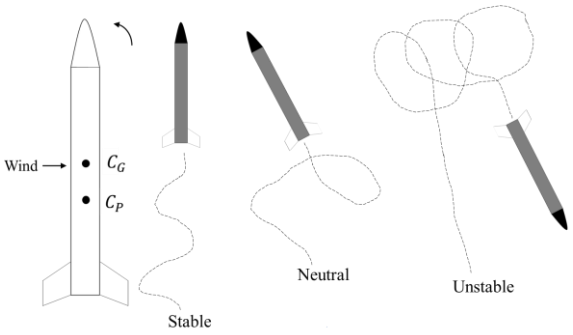

Fig. 1 Rocket stability.

where$C_P$and $C_G$are, respectively,the centres of pressure and gravity measured from the tip of the nose cone, and d is the diameter of the rocket body. From this equation, the static margin of the rocket depends on its centre of gravity and its centre of pressure. The centre of pressure is a single point at which all the aerodynamic forces are concentrated, while the centre of gravity is the average location of the weight of the rocket. There are a few factors that contribute to static margin, such as fins (wrap-around fin (WAF), fixed fin, and folded fin), canards, and active control fins.

For the rocket to be stable, there must be a distance of at least a diameter of the body between the centre of pressure and the centre of gravity[7]. If the centre of pressure and the centre of gravity are too close to each other, the rocket may be dynamically underdamped [8]. Likewise, if the distance between the centre of pressure and the centre of gravity is too great, the rocket becomes unstable, which may cause it to fall. For the rocket to make a stable flight, the centre of pressure must be behind the centre of gravity[9].

It is crucial for any flying object to identify the centre of pressure. The position of the centre of pressure in relation to the centre of gravity must be known to assess a rocket's static margin. The rocket might be classified as the lowest altitude rocket group out of the three sounding rocket classes, capable of reaching below 100 km altitude, based on its launching capabilities and altitude records. Therefore, it is more suitable to study low-altitude rockets than high-altitude rockets that can reach above 100 km in altitude.

The shape of the fins, fin semispan, and fin thickness are found to be the most important factors in determining the rocket’s static margin [10]. Triangular, trapezoidal, swept, and clipped delta fins were investigated in their study, along with four others regularly used fin designs. Furthermore, a fin's profile can help reduce drag while still allowing for useful lift forces. In terms of fin profiles, a tapered air foil that is symmetrical about its chord centre is the most efficient. Another discovery was that wrap-around fins exhibit less drag at greater angles of attack. Wrap-around fins can alsoenhance the longitudinal static margin and aerodynamic properties.

Previous study was conducted on the effect of fin form, fin thickness, fin number, and fin semispan on rocket static margin [11]. There was also research into how the fin design affects low-altitude rocket behaviour and static margin [12]. Recent research [13] investigated on the static stability of a model rocket. To determine the static stability of a model rocket, the study examined the capabilities of a simplified method, an analytical calculation, a graphical method, and several practical approaches, as well as the error of their application. They discovered that when creating model rockets, the simplest and most trustworthy way to figure out a rocket's static stabilityis by determining the center of pressure from the model drawing (from a flat figure). It is recommended to use it to launch demonstration rockets with a 15% or greater acceptable misalignment error. For building rocket sports models with demanding flight requirements, such as those for international competitions, analytical methods are useful. Previously, the study of the flight performance of notched delta-wing rockets on various types of nose cones was carried out [7]. The results reported that conical nose cones provide the most static margin when compared to parabolic, power, and hack series nose cones. However, it was discovered that the flying performances of parabolic and power-nosed model rockets performed better than conical-nose rockets. This occurred due to the conical nose cone's flat and sharp edges.

A study was conducted to determine the aerodynamic force and moment coefficients for the developed rocket[14]. According to this study, the total drag of the rocket is primarily attributed to the body, with the drag caused by the wrap-around fins accounting for only about 18.45 percent. A researcher investigated the aerodynamic properties (particularly the side force and rolling characteristics) to examine the effects created by different parameters of wrap-around fins and discover the associated mechanism [15]. The authors discovered that the drag generated by the wrap-around fins accounted for just about 7.42 percent of the total drag of the rocket. Both publications discovered similar findings: wrapped-around fin configurations can considerably increase the longitudinal static margin and the longitudinal aerodynamic characteristics of the entire rocket. It was additionally discovered that the extra side forces and rolling moments are mostly caused by unequal pressure distributions on both sides of the fins (windward or leeward). Besides, a study was conducted to investigate the effects of fin and nose cone shapes on rocket static margin and drag[12]. The authors found that the clipped triangular fin rocket gives the highest static margin among other types of fin design, and the best design in terms of the lowest drag force is the elliptical fin and ogive nose cone. This finding is further corroborated by more recent research[16], where the author uses traditional clipped delta fins for their model rocket. However, they also reported that the shape of the nose cone also affects the static margin. For example, when a conical nose cone is used, an elliptical fin produces the highest static margin. They also reported that the elliptical fin produced the lowest drag due tohaving the lowest frontal area of the fins among other designs.

Furthermore, another study was conducted on the influence of thrust deflection and centre of gravity deviation on the rocket's static motion margin [17]. The deviation of the falling points is shown to be almost linearly and sinusoidally depending on how the disturbance components interact with one another, increasing or decreasing the influence of the remaining parameters on the rocket's static motion margin. Control and static margin of a rocket plane was studied[18]. They discovered that the simultaneous deflection of all moving tails and the elevens is the most effective design of control surface deflection at subsonic speeds. The efficiency of the control surface's deflection increased as the Mach number grew. In addition, previous research was conducted to achieve an apogee of 2000 metres or higher with a total length of less than 1 metre and a weight of less than 750 grammes by developing a model rocket [19]. The finding is that a model rocket with an apogee of 2053 m can be launched legally, making it easier for rocket enthusiasts and students to learn about rocketry and flight patterns. The OpenRocket programme [20], [21], was utilised to calculate the rocket's centre of pressure and centre of gravity.

Previous studies on the flight and aeroelastic static margins of a small, lightweight rocket for transporting small payloads to high altitudes were also done [22]. The authors discovered that the study implies that the low aspect ratio fins under consideration can be made very thin. The vehicle's high-detail model yields a greater value of fin thickness than a simple discrete model. However, flight static margin may not be the limiting issue in their design. The optimisation of flight static margin and performance conditions for water rockets was performed using a statistical optimisation method [23]. The flying conditions for determining flight distance were discovered to be as follows: an initial air pressure of about 5 to 7 atm, a water volume ratio of about 30% to 40% of the bottle capacity (1.0 to 1.5 L), an aircraft weight of 100 to 130 g, and a launch angle of about 45 to 55. Furthermore, the requirements for stabilising the rocket's motion were studied before [24]. The author discovered that gravity affects the static margin regions for the beginning phase of burning, but not those for the final phase of burning.

Another study used moving mass control (MMC) to solve the problem of aerodynamic rudder control insufficiency caused by the low density of the upper atmosphere, reduce the aerodynamic thermal load of a high-speed missile, and address the issue of rudder surface ablation [25]. They discovered that when the spinning rate of the fast-spinning missile rose, so did the system's static margin region. A previous researcher also spent time on developing a finless model rocket [26]. The author discovered that a static margin could be obtained by weighting the nose sufficiently to transfer the centre of gravity away from the centre of pressure. To ensure a static margin, the proper weight-carrying engine needed to be used. Although the lack of fins appears to minimise drag on the vehicle, drag is enhanced because the cone creates a more tubulent wake. Aerodynamic flight was quite steady, having a nominal trajectory for a vertical flight with very minimal pitch. Several zero-drag characteristics were calculated and compared to positive drag predictions and actual altitude values. Mass ratio, burnout velocity,

burnout altitude, coast altitude, and total altitude were among those computed. Previous research studied a spinning rigid body and a particle with internal motion under axial thrust [27]. The results of this research show that the transition from asymptotically stable to unstable can occur at only two system frequencies. The above article is a fascinating example of a study about rocket static margin and rocket geometry.

The Astra rocket launch [28], which failed to reach orbit, and the Long March-5B rocket [29], which crashed into the Pacific Ocean, are two examples of unsuccessful rocket launches due to static margin concerns. The Astra rocket had a difficulty with the second rocket near the site of the launch failure. The Astra rocket's fairing covers are malfunctioning, spinning the payload, and causing it to burn up in the atmosphere. The Long March-5B rocket also re-entered the atmosphere over the Pacific Ocean in a separate occurrence. In contrast to previous rockets, the core stage of the Long March 5B rocket is sent into orbit in its whole and spends several days circling the Earth. It finally experiences orbital instability and falls to Earth.

Generally, various stresses and disturbances were applied to the rocket during the flight. So, the static margin aspect must be defined to recover and protect the rocket. The location of the centre of gravity and the centre of pressure in a rocket determines its static margin. A restoring moment will not be produced by the rocket's drag force if the centre of pressure is ahead of the centre of gravity[16]. In flight, the rocket trembles because of that. The rocket will become unstable and will probably start to "weathercock" as it rises if the gap between the centre of pressure and the centre of gravity is too great [14]. It is crucial to employ an appropriate procedure to determine the location of the centre of gravity and the centre of pressure. Computational methods are more practical than experimental procedures, especially for larger rocket motors, when identifying the locations of the centres of pressure and gravity. Most amateur rocket builders assess the static margin of their rockets using the OpenRocket software, which solves Barrowman equations[30] to estimate the location of the centre of pressure. This is because experimental approaches to identifying the location of the centre of pressure are relatively difficult.Alternatively, one can employ computational fluid dynamics methods that are more convenient[16]than the experimental approach. However, the CFD approach requiresrelatively more computing power and technical knowledge, which might not be accessible toamateur builders. Hence, validating the OpenRocket data is rather crucial, knowing that the results are derived from simple mathematical equations, i.e., the Barrowman equations. However, to the best of the authors' knowledge, a study to validate the OpenRocket software is yet to be conducted, particularly in terms of its capacity to forecast the location of the centre of pressure. Hence, the goal of this study is to evaluate the accuracy of the OpenRocket software in predicting thestatic margin of a low-altitude rocketwith various fin designs. Specifically, the research aimed at evaluating thecentre of pressureof a low-altitude rocket flying at an average speed of 300 m/susing computational fluid dynamics and comparingthe data with mathematical predictions from OpenRocket.

This study is hoped to furnish valuable information on the accuracy of the Barrowman equations in terms of predicting the centre of pressureof the rocket.

Methodology

In the present study, a computational approach was employed to determine the centre of pressure of a rocket with various fin semispans and thicknesses. The fin has a clipped deltaplanform, and the sweep length is fixed while varying the semispan (i.e., the root and tip chords are kept constants for all cases). The rocket has a body diameter of 16 cm. The fin semispan is varied by 0.3125, 0.625, 0.9375, 1.2, 1.5625, and 1.875, while the thickness is varied by 0.0125, 0.015625, 0.01875, and 0.021875. All variables are expressed in a non-dimensional form with a characteristic length scale equal to thediameter of therocket body, unless otherwise mentioned. First, the centre of pressure is approximated using Barrowman equations, which are presented in detail in the following section. The equations were solved using theopen-source software OpenRocket. Next, the centre of pressure is predicted by solving the Navier-Stokes and continuity equationsby means of computational fluid dynamics simulations. A 3Drepresentation of the rockets was modelled using computer-aided design (CAD) software, which was then meshed and analysed in an OpenFOAMcomputational fluid dynamicspackage. The following section detailsthe mathematical predictionsfor estimating the centre of pressure of the rocket.

A. Estimation of centre pressure using Barrowman equations

Barrowman equations (equations (2)-(9)) were used to estimate the location of the centre ofpressure for a given rocket geometry. The computation is typically broken down into fourregions: the nose, conical shoulder, conical boattail, and fins. Equation (2) was used to calculate the centre of pressure of the rocket, i.e.,

$$\bar{X} = \frac{((C_N)_n \bar{X}_n + (C_N)_{CS} \bar{X}_{CS} + (C_N)_{cb} \bar{X}_{cb} + (C_N)_{fb} \bar{X}_f}{C_N}. \quad (2)$$

However, the rocket in the present study does not contain a conical shoulder or conical boattail. Therefore, equation(2) reduces to the following:

$$\bar{X} = \frac{((C_N)_n \bar{X}_n + (C_N)_{fb} \bar{X}_f}{C_N}. \quad (3)$$

Subscripts in symbols represent specific rocket regions they relate to. For instance, $(C_N)_n$ represents the force on the nose of the rocket. Symbols without subscripts refer to the entire rocket. This study uses subscripts such as*f*, *fb*, and *n* to denotefins, fins in the presence of the body, and nose, respectively. The geometrical definition of a typical rocket is depicted in Fig.2.

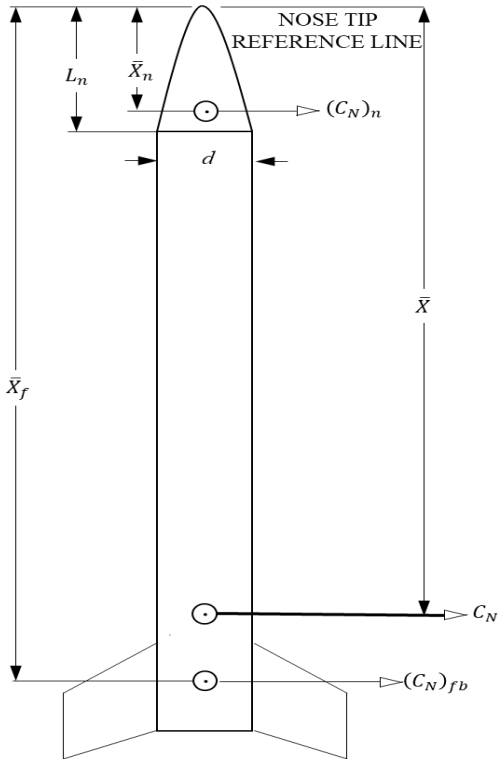

Fig.2 Geometrical definitions of a typical rocket.

In general, the normal force coefficient on the nose, $(C_N)_n$, is identical for all shapes and always has a value equal to two[31]. On the other hand, the centre of pressure location on the nose varies with each different nose shape. In this study, an ogive nose was used. For an ogive nose cone, the distance from the tip of the nose to the centre of pressure is $X_N = 0.466L_n$, where L_n is the nose cone length[31].

Fig. 3 shows a generalised fin shape. The force on the fins of a rocket with n fins was calculated using equation (4).

$$(C_N)_f = \frac{4n(\frac{S}{d})^2}{1+\sqrt{1+(\frac{2\ell}{a+b})^2)}}, \qquad (4)$$

where the number of identically shaped fins, n, was 4.S, ℓ, a and b refer to the fin semispan, the length of the fin mid-chord line, the fin root chord, C_R, and the fin tip chord, C_T, respectively.In addition, the air flow over the fins is somewhat influencedby the air flow over the body section to which the fins are attached. To account for this, the fin forces for four fins are multiplied by an interference factor in equation (5).

$$K_{fb} = 1 + \frac{R}{S+R}, \qquad (5)$$

where R is the radius of the body between the fins, as shown in Fig. 3. The total force on the tail in the presence of the body was calculated using equation (6), i.e.

$$(C_N)_{fb} = K_{fb}(C_N)_f. \qquad (6)$$

The fin centre of pressure is in the same place on any two fins of the same size and shape. Since all the fins on a particular stage of a rocket are the same size and shape, the centre of pressure location of the tail does not depend on the number of fins, as shown in equation (7).

$$\bar{X}_F = X_f + \Delta X_f, \qquad (7)$$

$$= X_f + \frac{m}{3}\frac{(a+2\mathrm{b})}{(a+b)} + \frac{1}{6}[(a+\mathrm{b}) - \frac{(ab)}{(\mathrm{a}+\mathrm{b})}],$$

where X_f is the distance from the nose tip to the front edge of the fin root, as shown in Fig.2.

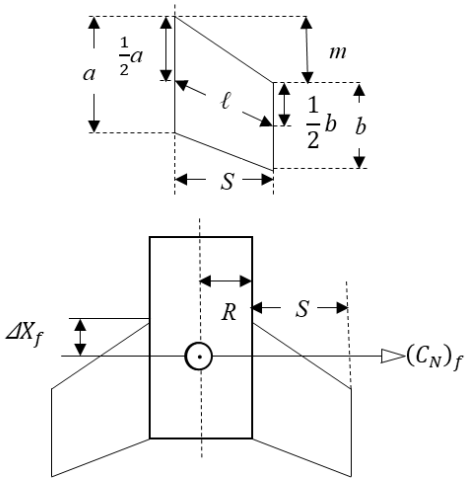

Fig. 3Geometrical definitions of a typical rocket fin.

The total force on the entire rocket is the sum of all the forces on the separate regions, which was calculated using equation (8).

$$C_N = (C_N)_N + (C_N)_{cs} + (C_N)_{cb} + (C_N)_{fb}. \quad (8)$$

However, as mentioned earlier,the conical shoulder and boattail are neglected in this study; hence, $(C_N)_{cs}$ + $(C_N)_{cb}$is set to 0.Therefore, the final total force on the entire rocket is shown in equation (9).

$$C_N = (C_N)_n + (C_N)_{fb}. \quad (9)$$

Equation(2) can be easily solved usingExcel spreadsheets. However, open-source software such as OpenRocket offers greater functionalityand the capacity to fine-tune rocket designs based on real-time performance feedback.The software is also used to evaluate other rocket performances, such as drag and flight performance. Using this software, individual regions can do their own custom overrides for materials, weights, dimensions, and other factors. The properties of the materials that were acquired before can then be incorporated into the model. Static margin-focused design is also made easy by the software. The positions of the centre of pressure and gravity are adjusted each time a component is added to reflect the new information. This analysis ensures the development of a rocket with stable flight.

B. 3D modelling

A 3D representation of the rockets was modelled using CAD software.
Fig.4 shows a typical 3D model of the rocket investigated in the present study.The type of fins used is a clipped delta fin, the rocket body diameter is 1, the sweep length is 0.3125, the tip chordis 1.125, the root chordis 1.4375, and the number of fins is 4. The fin semispanvaries between 0.3125 and 1.875,while the fin thickness varies

between 0.0125and 0.021875. All length dimensions are non-dimensionalised by the rocket body diameter, which is 16 cm.

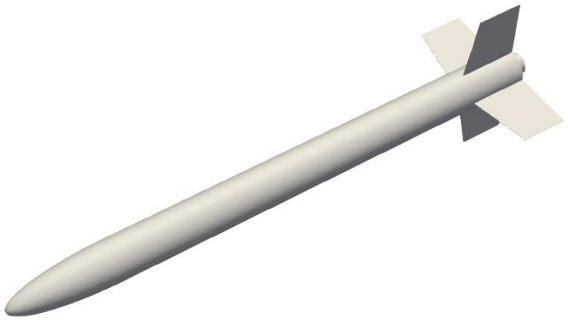

Fig.4 3D representation of a rocket analysed in the present study.

C. Computational Fluid Dynamics analysis

Utilising the computational fluid dynamicssoftware, the pressure distribution around the rocket body (including the nosecone and fins) was integrated to find the rocket's centre of pressure, i.e.,

$$C_{P,x} = \frac{\int x\, p(x)dx}{\int p(x)dx}, \qquad (10)$$

where $C_{P,x}$ is the rocket's longitudinal centre of pressure, x is the longitudinal location, and $p(x)$ is the local pressure. A typical pressure distribution on the rocket surface is depicted in
Fig.5.

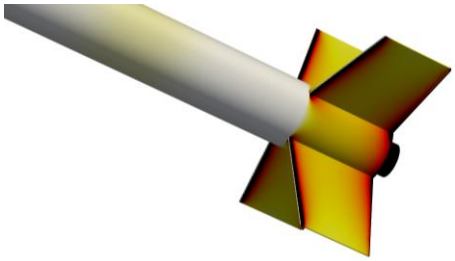

Fig.5 Typical pressure distribution on the rocket fin surface at zero angle of attack. The dark and light regions represent low and high surface pressure, respectively.

A high-resolution meshing configuration was constructed, particularly in the area near the physical surfaces, to capture any expected strong velocity gradient.The computational domain is modelled as a disc plate, as shown in Fig. 6,with a diameter and thickness of, respectively,318 and 18.75, both non-dimensionalised using the rocket body diameter. The domain size is considered sufficiently large to eliminateboundary effects[32]. The inlet plane

was set to a streamwise velocityof 300 m/s. The surrounding temperature and pressure areset to be 305 K (32 °C) and 100 kPa, respectively. The simulations were conducted for a sufficient time to allow for fully developed flows and the centre of pressures were calculated while excluding the transient part of the simulation data.

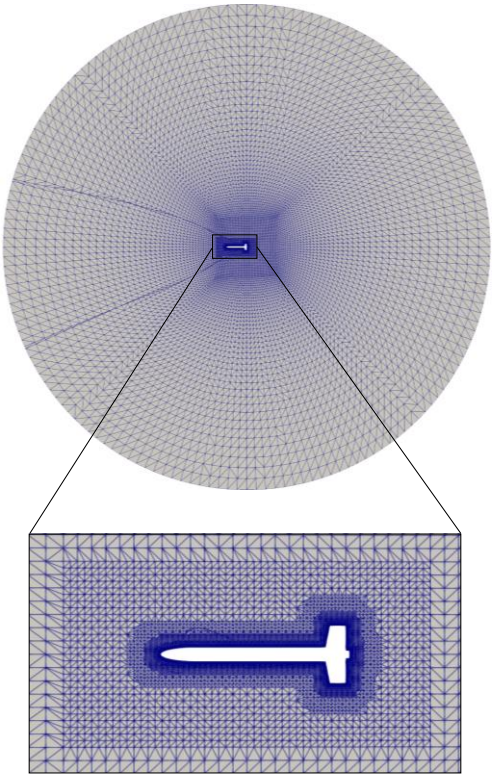

Fig. 6Computational domain with magnified mesh in the vicinity of the rocket

Kurganov's scheme was employed as the flux scheme, which is a second-order high-resolution central difference scheme. For time advancement, the Euler implicit method was applied. The gradient terms were discretised by the Gauss linear scheme.

I. RESULTS AND ANALYSIS

Fig. **7** shows a plot of thecentre of pressure and centre of gravity against the fin semispan from the mathematical predictions using Barrowman equations.The centre of gravity varies almost linearly with the fin semispan, regardless of the fin thickness.This observation is expected since the volume (and thus the weight, assuming homogeneous material) of the fin with trapezoidal planform increases linearly with fin semispan, i.e.

$$V = \frac{1}{2}(a + b)St. \tag{11}$$

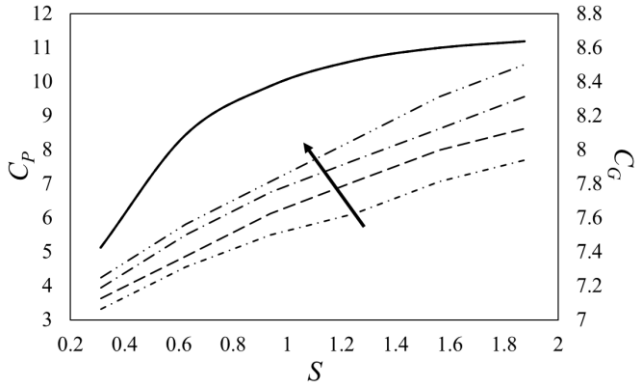

Fig. 7The centre of pressure and centre of gravity are plotted against the fin semispan. A solid line represents the centre of pressure data for different fin thicknesses, which collapses into a single line. Non-solid lines represent centre of gravity data, where the direction of the arrow represents the increase in fin thickness.

It can also be seen from
Fig. 7that the distance of the centre of pressure from the nose cone increases linearly up to a fin semispan of approximately 0.6 (60% of the body diameter). Further increasing the fin semispan beyond this value resulted in a more subtle change of the centre of pressure, and it appears to asymptote towards a constant value. This observation is attributed to the fact that the centre of pressure and the centre of gravity shifted downward towards the tail of the rocket simultaneously as the fin semispanincreased.

Furthermore, it is interesting to note that the curve of the centre of pressure data for different fin thickness collapses into almost a single line, indicating the fin thickness has little effect on the centre of pressure. This finding agreeswith a previous study, where it was found that the thickness of the clipped delta fin effects only 0.5% of the rocket's stability compared to another fin's parameters, such as root chord, tip chord, and semispan [10].
Fig. **8**shows a plot of static marginagainst fin semispan at various fin thicknesses.It is to be noted that the static margin is the distance between the centre of pressure and the centre of gravity, as indicated in equation (1). The trend of the static margin with various fin semispan almost coincides with that of the corresponding centre of pressure. It is therefore deduced that the variation of the rocket's static margin withfin semispan is governed by the centre of pressure.

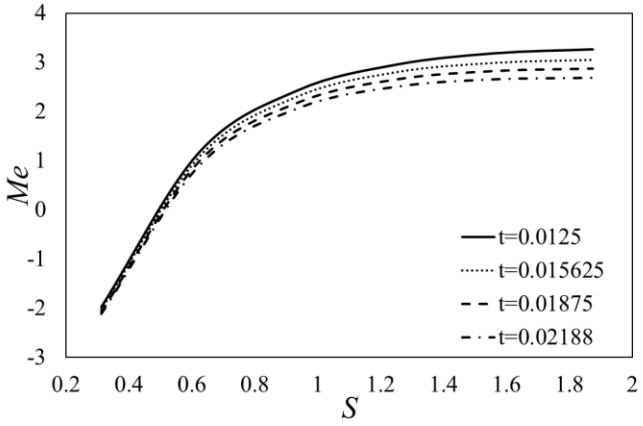

Fig. 8 Static margin plotted againstfin semispan with variousfin thicknesses.

It is also noted from

Fig. **8**that the variation of the static margin with the fin thickness is more prominent at a larger fin semispan. This is due to the increase of the fin volume-fin semispan gradient with fin thickness, as shown in Fig. **9**, resulting in a more significant increase in fin mass and thus the shift of the centre of gravity. Mathematically, it can be shown that the fin volume-fin semispan gradient is proportional to the fin thickness by integrating equation (11) with respect to the fin semispan, i.e.,

$$\frac{dV}{dS} = \frac{1}{2}(a + b)t. \qquad (12)$$

In the present study, the fin has a constant fin root and tip chord length;thus, it is shown that,

$$\frac{dV}{dS} \alpha\ t. \qquad (13)$$

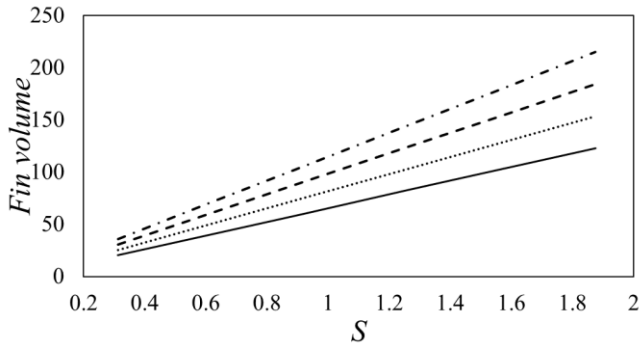

Fig. 9Fin volume plotted against fin semispan at various fin thicknesses.The line legend is the same asthat in

Fig. 8.

Fig. **10**shows a plot of thecentre of pressure andcentre of gravity against thefin semispan from the mathematical predictions and computational fluid dynamics simulations. TheCFDdata predicts a linear relationship between thecentre of pressure and fin semispan, while mathematical predictionspredict alogarithmic relationship between thecentre of pressure andfin semispan.

The difference in trend between mathematical andCFD predictions is likelydue to the assumptions made in the mathematical predictions.The Barrowman equations are also valid for a rocket speed that is much less than the speed of sound, i.e., below 180 m/s. In the present study, the rocket flight was simulated at a speed of 300 m/s. The equation also assumed that the air flow over the rocket is smooth and does not change rapidly [31], while in actual the boundary layer flow over the rocket might be turbulent, particularly when the rocket is flying at a high speed.

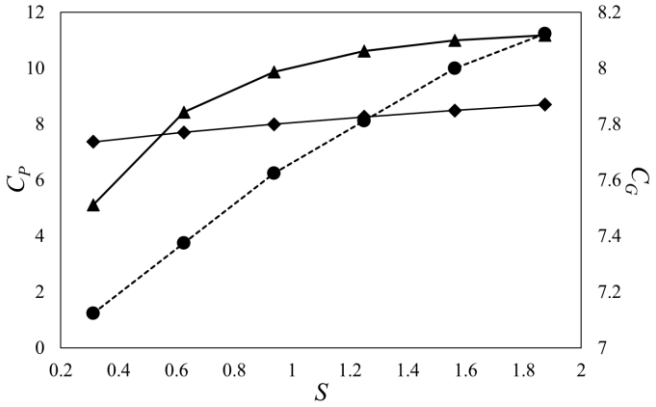

Fig. 10The centre of pressure andcentre of gravity areplotted against thefin semispan.The triangle and diamond markersrepresent, respectively,mathematical, and computational fluid dynamics predictions of the centre of pressure (primary vertical axis). Theround marker represents the centre of gravity (secondary vertical axis).

Fig. **11**shows a plot of static marginagainst fin semispan from the mathematical predictions and CFD simulations.It is to be noted that the static margin data for CFDis derived from equation(1) using the centre of gravity calculated by OpenRocket software. Again, it is observed that the trend of the static margin with various fin semispan predicted by CFD almost coincides with that of the corresponding centre of pressure. Hence, the deduction that the centre of pressure governs the variation of the rocket's static margin with fin semispan is confirmed.

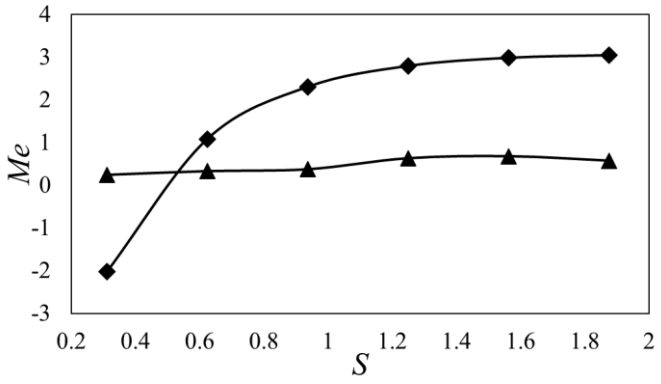

Fig. 11Static margin plotted against the fin semispan graph. The diamond and triangle markers represent mathematical predictions and computational fluid dynamics, respectively.

Conclusion

Static margin data obtained from mathematical predictions and CFDwas compared. Numerous investigations were conducted to examine various relationships, including the relationship between the static margin and fin semispan, the centre of pressure andfin semispan, and other relevant relationships. It can be concluded that the influence of the fin thickness on the centre of pressure is negligible across all evaluated fin semispans, whereas the centre of gravity is determined by the fin's weight. Furthermore, it is noted that the CFD and mathematical predictions of the centre of pressure differ, with the former predicting a linear relationship with fin semispan and the latter predicting a logarithmic relationship. However, the CFD data confirmed the mathematical predictions that the centre of pressure governs how the static margin of the rocket changes with fin semispan. Although thefin

thickness has minimal impact on the centre of pressure, the static margin exhibits variation in relation to the thickness of the fin as the fin semispan is increased.There were inconsistencies noted between the computational fluid dynamics (CFD) data and the mathematical predictions obtained usingBarrowman equations. These disparities warrant additional scrutiny and perhaps necessitate adjustments to the Barrowman equations.

Acknowledgement
This publication was supported by the Strategic Research Partnership grants 100-RMC 5/3/SRP PRI (024/2020)) and (100-RMC 5/3/SRP (020/2020) and Micro-Industry Hub (MIH) Program (MIH-(005/2020)), a funded program under Universiti Teknologi MARA and MTC Engineering Sdn Bhd.This publication was alsosupported by Dermasiswa Yayasan Perak, which provides one-off start-up assistance for students to continue their studies at the university or IPT level in the country and abroad, and Perbadanan Tabung Pengajian Tinggi Nasional (PTPTN), which is a government institution that offers study loans specifically for tertiary education for Malaysian students.

References

[1] J. Huh and S. Kwon, “A practical design approach for a single-stage sounding rocket to reach a target altitude,” Aeronautical Journal, vol. 126, no. 1301, pp. 1084–1100, 2022, doi: 10.1017/aer.2022.18.

[2] A. N. Barbosa and L. N. F. Guimãraes, “Multidisciplinary design optimization of sounding rocket fins shape using a tool called mdo-sonda,” Journal of Aerospace Technology and Management, vol. 4, no. 4, pp. 431–432, 2012, doi: 10.5028/jatm.2012.04044412.

[3] A. Garcia and G. Da Silveira, “Proposal of Static Margin Limit during Launch Phase for the VS-30 Orion Sounding Rocket,” SAE Technical Papers, vol. 2015-Septe, no. September, 2015, doi: 10.4271/2015-36-0160.

[4] V. Lorenzo, “Static and Dynamic Analysis of the Aerodynamic Stability and Trajectory Simulation of a Student Sounding Rocket,” pp. 1–130, 2014.

[5] S. Shah, N. Tanwani, S. K. Singh, and M. Makwana, “Drag Analysis for Sounding Rocket Nose Cone,” International Research Journal of Engineering and Technology, no. July, pp. 2393–2397, 2020, [Online]. Available: www.irjet.net

[6] A. H. Abdul Hamid, Z. Salleh, A. M. I. A. Suloh, M. J. Sujana, M. S. Saad, and M. I. Khamis, “Evaluation of a Newly Designed Aerodisk for Cloud Seeding Prototype Rocket Drag Reduction,” Pertanika J Sci Technol, vol. 30, no. 2, pp. 1409–1419, 2022, doi: 10.47836/pjst.30.2.31.

[7] M. O. Cihan OZEL, Cevher Kursat MACIT, “Investigation of Flight Performance of Notched Delta Wing Rockets on Different Types of Nose Cones,” vol. 18, no. 2, pp. 435–447, 2023.

[8] S. Negahban, “Design of a Model Rocket Flight Logging System and In-Air Deployable Rover Design of a Model Rocket Flight Logging System and In-Air Deployable Rover,” 2019.

[9] A. Yarce, J. Sebastián Rodríguez, J. Galvez, A. Gómez, and M. J. García, “Simple-1: Development stage of the data transmission system for a solid propellant mid-power rocket model,” J Phys Conf Ser, vol. 850, no. 1, 2017, doi: 10.1088/1742-6596/850/1/012019.

[10] A. Pektas, U. Haciabdullahoglu, N. Ejder, Z. Demircan, and C. Tola, “Effects of different fin shapes on apogee and stability of model rockets,” Proceedings of 9th International Conference on Recent Advances in Space Technologies, RAST 2019, no. August, pp. 193–199, 2019, doi: 10.1109/RAST.2019.8767439.

[11] A. Hussein Abdul Hamid et al., "The Effect of Different Designs of Fins and Nose Cones towards the Stability and Performance of a Sugar Rocket," International Transaction Journal of Engineering, vol. 13, no. 13, pp. 1–14, 2022, doi: 10.14456/ITJEMAST.2022.261.

[12] R. Ujjin, S. Chaikiandee, and C. Ngaongam, "Low Altitude Local Rocket Aerodynamics Analysis and Experimental Testing †," 2021.

[13] V. A. Bordachev, V. V. Kolga, and E. A. Rozhkova, "Static stability study of a model rocket," Siberian Aerospace Journal, vol. 24, no. 1, pp. 64–75, 2023, doi: 10.31772/2712-8970-2023-24-1-64-75.

[14] A. Eltaj, M. Ahmersheen, S. Babikir, and H. Abudarag, "Aerodynamic analysis of (GRAD (Rocket using (CFD) تحليل الديناميكا الهوائية للصاروخ (GRAD) الموائع التحسيبية ديناميكا باستخدام," 2019.

[15] S. C. M. Y. J. S. Guo Qing Zhang, "Aerodynamic characteristics of a wrap-around fin rocket," Jan. 04, 2016.

[16] H. Prasanna Manimaran, G. Kompelli, and L. Khaja Naib Rasool Shaik, "Stability Analysis of Conventional Rocket Model using CFD Tool," 2020. [Online]. Available: www.ijert.org

[17] H. B. Le and P. Konečný, "Effect of some disturbance factors on the motion stability of unguided rockets," Advances in Military Technology, vol. 15, no. 2, pp. 405–423, 2020, doi: 10.3849/aimt.01379.

[18] A. Kwiek, "Study on Control and Stability of the Rocket Plane to Space Tourism," 2014. [Online]. Available: https://www.researchgate.net/publication/285733392

[19] R. Nanditta et al., "Structural Design and Analysis of High-Powered Model Rockets using Open Rocket," International Journal of Engineering Research in Mechanical and Civil Engineering (IJERMCE), vol. 6, no. 8, pp. 64–68, 2021, [Online]. Available: https://www.researchgate.net/publication/353999315

[20] S. Niskanen, "Development of an Open-Source Model Rocket Simulation Software," p. 111, 2009.

[21] S. Niskanen, "Open Rocket technical documentation Sampo Niskanen," pp. 1–118, 2010.

[22] D. J. Mctavish, D. R. Greatrix, and K. Davidson, "Unconstrained flight and stability analysis of a flexible rocket using a detailed finite-element based procedure," 2005. [Online]. Available: www.witpress.com,

[23] Y. I. Eiji Toma, "The Method for Optimum Design of Water Rocket Flight Stability Performance Conditions Using CAE with T Method and Robust Parameter Design," 2021.

[24] T.N. Srivastava & Manak Singh, "7407-Article Text-18954-1-10-20140522".

[25] Qiushi Zheng and Zhiming Zhou, "Stability of Moving Mass Control Spinning Missiles with Angular Rate Loops," Nov. 2019.

[26] T. Dombeck, "A Study on Conical Rocket Stabilization," 1973.

[27] F. L. Janssens and J. C. Van Der Ha, "Stability of spinning satellite under axial thrust and internal mass motion," Acta Astronaut, vol. 94, no. 1, pp. 502–514, 2014, doi: 10.1016/j.actaastro.2012.09.013.

[28] Scott Heidler, "Astra's failed rocket launch reminds us spaceflight can be difficult," Jun. 14, 2022. https://www.wesh.com/article/astra-rocket-failure/40278588 (accessed Jan. 05, 2023).

[29] Christian Davenport, “Chinese rocket tumbles into Pacific Ocean after days in space,” Nov. 04, 2022. https://www.washingtonpost.com/technology/2022/11/04/china-rocket-long-march-earth/ (accessed Jan. 05, 2023).

[30] J. S. Barrowman, “The Practical Calculation of the Aerodynamic Characteristics of Slender Finned Vehicles,” no. March, p. 103, 1967.

[31] J. Barrowman, “Technical Information Report Calculating the Centre of Pressure .pdf,” 1988.

[32] S. Zhu, Z. Chen, H. Zhang, Z. Huang, and H. Zhang, “Investigations on the influence of control devices to the separation characteristics of a missile from the internal weapons bay,” Journal of Mechanical Science and Technology, vol. 32, no. 5, pp. 2047–2057, 2018, doi: 10.1007/s12206-018-0414-3.